



Semnan University

Mechanics of Advanced Composite Structures

journal homepage: <http://MACS.journals.semnan.ac.ir>

Experimental and Numerical Investigation on the Flexural Behavior of Composite-Reinforced Top-Hat Shape Beam

N. Zahedan ^a, H. Ahmadi ^{a*}, G.H. Liaghat ^{a,b}

^a Faculty of Mechanical Engineering, Tarbiat Modares University, Tehran, Iran

^b School of Mechanical & Aerospace Engineering, Kingston University, London, United Kingdom

KEYWORDS

Top-hat section beam
Composite reinforcement
Three-point bending test
LS-DYNA
Specific energy absorption

ABSTRACT

Top-hat hollow-section beams are widely used in passenger vehicle's body-in-white structure because of their proper shape for the montage process and also crashworthiness advantages. Hollow section beams with top-hat cross-section are mostly employed in structures like B-pillar, rocker sill, and roof rail which are engaged in side impact collisions. In the present investigation, simplified top-hat beams are developed based on a conventional B-pillar with the aim of improving energy absorption characteristics. Reinforcements are conducted by employing fiber glass-epoxy composite material. Three types of reinforced beams are presented which are either improved by composite-laminating, or by installation of an extra composite-made internal reinforcement. Experimental tests are performed in quasi-static three-point bending condition and based on results, a FE simulation is developed using LS-Dyna explicit code. Specimens are compared based on peak load, total energy absorption (TEA) and specific energy absorption (SEA) amounts. Also, to illustrate the extent of improvements, a not-reinforced top-hat beam is experimentally subjected under three-point bending test. Results depict a significant difference between the performance of beams reinforced by different methods. Comparison between specimens, considering their respective load-displacement diagram and crashworthiness characteristics, show that applying composite laminates to the inside surface of a hat-shaped beam would produce a beam with satisfying flexural behavior.

1. Introduction

Safety of passengers in vehicle collisions was an essential consideration since automobile industry was developed. Before performing final realistic crash tests for safety ratings, main structures of a vehicle is designed based on required strength and crashworthiness optimization. Thin-walled structures are widely used in passenger vehicle's body-in-white. Among all various cross-sections which have been proven to have great effects on the energy absorbing capabilities of the thin-walled extrusions, top-hat and double-hat profiles have been widely applied on structures of chassis in the past few decades since their geometrical features are suitable for fast production using spot-welding techniques and their acceptable performance in flexural loadings [1]. Strengthening and improving energy absorption characteristics of these thin-walled tubular

beams has been aimed by many researchers to promote safety rating of automobiles. Metallic cellular materials which have a high crushing resistance to weight ratio, such as closed-cell aluminum foams and honeycombs, were chosen as an ultra-light metal core in reinforcing thin-walled tubes [2-5]. Moreover, employing polymeric materials such as polyurethane foam is proven to have a significant effect on energy absorption characteristics of tubular beams [6]. Chen et al. [7] investigated the bending collapse of thin-walled beams filled with aluminum foam and aluminum honeycomb. The specific energy absorption of foam and honeycomb filled beams were found about 60 to 115% higher than non-filled beams. On the other hand, in the automotive industry, a reduction of the weight of the structures' constituents improves vehicle's performance and fuel economy. A way to achieve an enhanced lightweight design in fundamental thin-walled chassis beams is to employ

* Corresponding author. Tel.: +98-21-82883391
E-mail address: h_ahmadi@modares.ac.ir

composite materials due to their high strength to weight ratio and specific stiffness. Many efforts have been made to investigate methods of using composite materials in practical applications. Researchers have done studies on externally fiber reinforced thin-walled tubes [8-13]. Lee et al. investigated bending deformation and energy absorption characteristics of aluminum-composite hybrid tube beams. Specific maximum moment and specific absorbed energy of beams increased by about 105% and 120% compared with empty tube beams, respectively [8]. Shin et al. investigated energy absorption capability and failure mechanisms of aluminum-hybrid square tube beams wrapped with glass-fiber reinforced plastics under bending collapse loads, and compared those results with calculation results from modified theoretical models. Theoretical calculation and experimental results were similar [11].

In passenger vehicles, the ability to absorb impact energy and to be survivable for the occupant is called the "crashworthiness" of the structure. There is an important difference between crashworthiness and penetration resistance. Crashworthiness is concerned with the absorption of energy through controlled failure mechanisms and modes that enable the maintenance of a gradual decay in the load profile during absorption. However, penetration resistance is associated with the total absorption without allowing projectile or fragment penetration.

This study is focused on improving structures involved in side collisions, such as B-pillar and rocker sill. Mentioned structures are represented using a beam consisted of a hat-shaped bar and a back-plate. A novel internal reinforcing component is suggested and manufactured using composite material. Performance of the reinforced beam is compared with similar beams reinforced by hybrid method and also a not-reinforced beam. Tests were performed experimentally under quasi-static three-point bending condition.

2. Experimental Procedure

Collision of vehicles are categorized as "low velocity" impact. Previous investigations have proven that mechanism of collapse in dynamic low velocity loading and quasi-static loading are the same. Moreover, results obtained from quasi-static tests are often more accurate and reliable for developing numerical simulations. Also, quasi-static tests are simple and easy to control while impact tests require very expensive equipment to follow the crushing process and measure the essential parameters because the whole crushing takes place in a split second. Hence, quasi-static tests are used to study the

failure mechanisms in composites, by selection of appropriate crush speeds. Therefore, a quasi-static test is preferred to investigate the energy absorption characteristics of specimens. Three-point bending tests were performed using a universal displacement-control machine in quasi-static condition as shown in Fig. 1. Speed of indentation was 5mm/min and span of specimens was 350mm.

According to the boundary condition of three-point bending test illustrated in Fig. 1, mechanism of collapse and formation of folds are only influenced by cross-section of specimens' components in area under the indenter. Therefore, a constant cross-section is used throughout specimens to represent B-pillars, and while curves are eliminated. Dimensions of full-scale specimens are adopted from the dominant cross-section in a conventional B-pillar. The length of a full-scale specimen would be about 665mm [14] thus it couldn't be fitted in the test machine. Similitude theory [15] is used to make sure the comparisons (based on peak load, EA and SEA) between specimens are valid and deformation modes will be the same in full-scale and scaled-down specimens. On this basis, specimens can be geometrically scaled by a constant ratio in three dimensions and if the scale factor is λ , forces are scaled by λ^2 and energies are scaled by λ^3 . Considering test device's dimensions and fabrication facilities, $\lambda = 0.53$ was chosen and sheet metal by thickness of 0.8 mm was employed to manufacture specimens instead of 1.5 mm plate in the real structure.

The basic components of the beams, which are the hat-shaped bar and back-plate, are fabricated using cold rolled stainless steel ST14 grade sheet plate. Fiber glass-epoxy material is selected for composite reinforcement parts.

Four types of specimens with the same overall shape and dimension were prepared for investigation. The C0 specimen had no reinforcement and only consisted of a metal top-hat and a back-plate but the others had fiber glass/epoxy composite laminate as reinforcement between the top-hat and back-plate. In C1 and C2 specimens the back-plate and the top-hat is reinforced, respectively. For better performance the composite reinforcement is cured as bound to the metal sheet which created a fiber metal laminate (FML). The C3 specimen had an individual triangular shape reinforcement as shown in Fig. 2. Also, a close-up image of hybrid cross-sections is illustrated in Fig. 3.

All composite sections are produced using 12 layers of woven fiber glass in 0° and 90° directions. Vacuum Assisted Resin Transfer Molding (VARTM) method was employed for fabrication of composite parts (Fig. 4). Fig. 5 shows the fabricated FML parts and Fig. 6

illustrates the process of fabricating of triangular reinforcement. A metal mold was designed to form the fiber composite laminate and after resin infusion, the composite laminate was separated from the mold and trimmed to the final shape. Finally, the components are fixed together by 20 M4 hexagon screws.

Total mass of an empty beam (without reinforcement) is about 590 g and the mass of reinforced specimens are equal to 721 g, 840 g, and 766 g for specimens C1, C2, and C3, respectively.



Fig. 1. Experimental setup for the quasi-static three-point bending tests.



Fig. 2. Fabricated specimens.

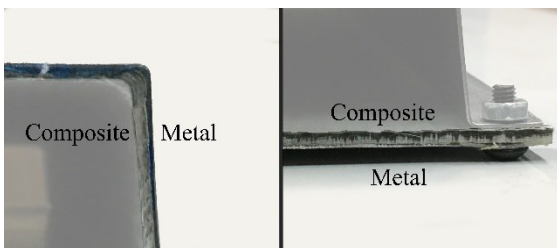


Fig. 3. Close-up image of cross-sections: (right) C1 and (left) C2.



Fig. 4. Vacuum assisted resin transfer molding.

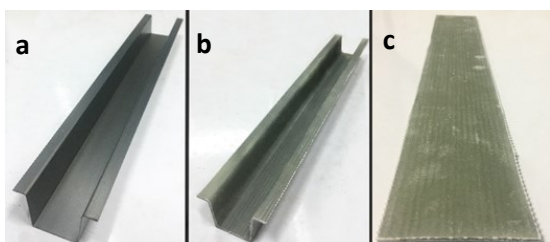


Fig. 5. Composite laminating process: (a) Metal top-hat, (b) inner laminated top-hat, (c) laminated back-plate.

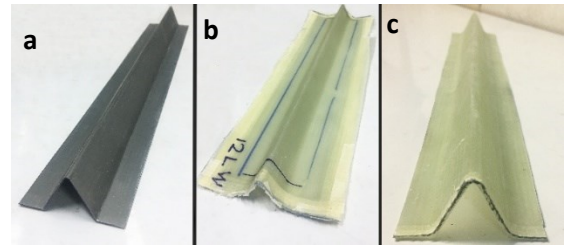


Fig. 6. Manufacturing of the triangular composite reinforcement: (a) metal mold, (b) composite specimen after resin infusion, (c) final product after trimming.

3. Numerical Simulations

The computer programs used for Finite element analysis (FEA) apply numerical methods in the estimation of the various mechanical properties of engineering designs that can withstand a set of loads [16]. Engineers are able to substitute physical testing with FEA solutions which have a direct effect on time and economics of engineering analysis and design.

Linear FEA has helped to solve real-life problems for many years while the expansions in engineering practices ensure that more sophisticated tools like non-linear systems are developed. Linear systems do not account for plastic deformation in engineering systems, although it is possible in non-linear systems. Non-Linear systems can often be used for material testing where the behavior of failure is to be examined. In this study, Finite element analysis (FEA) was performed using LS-DYNA explicit code [17] on a 64-bit Windows 7 workstation. The beam dimensions, indenter size and indenter speed were set to match the experimental test. Belytschko-Tsay shell elements were used (ELFORM=2) with hourglass formulation option 4. A mesh sensitivity analysis is performed to make sure that the selected mesh size provides the result of steady-state three-point bending force with relative error less than 1%. As a result, mesh size of 2.5×2.5mm was selected with quadrilateral shell elements.

The material in metal components of hybrid beam were modelled using material card No. 24 MAT_PIECEWISE_LINEAR_PLASTICITY and composite sections using No. 59 MAT_COMPOSITE_FAILURE_SHELL_MODEL.

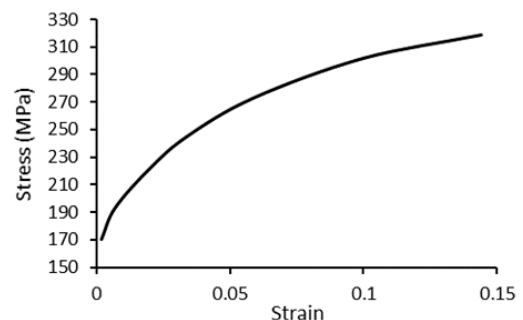


Fig. 7. Stress-strain curve used in material model No. 24.

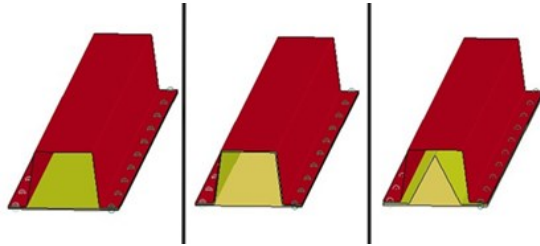


Fig. 8. Numerically simulated models.

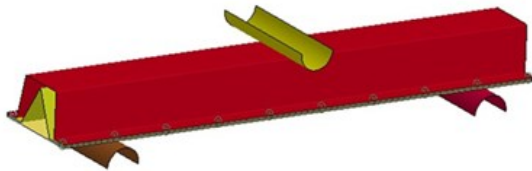


Fig. 9. Quasi-static three-point bending simulation.

Metal material predicts plastic deformation with lending itself to quick translation of experimental test data by describing the stress-strain curve as linear segments (eight data points were used). The curve is plotted in Fig. 7. Detail of material properties used for metal is listed in Table 1 which is extracted by performing ASTM E8 (standard test methods for tension testing of metallic materials). To provide instability of orthotropic properties during deformation in material model used for composite sections a local coordinate system is preferred over global coordinate to define the properties in three directions. Composite material inserts are listed in Table 2. Mat No. 59 is designed to predict behavior of a composite material by employing three-dimensional analysis. By defining material axes, values of tensile and shear modulus are used in respective directions. Since the thickness of composite laminates are about 1.9 mm and tests were conducted under flexural loading, no considerable delamination was observed in failure procedure of experimental specimens. Thus the chosen material model is programmed based on shell elements and damage is predicted using in-plane strength values. Also because of using woven glass fibers, the longitudinal and transverse strength values are equal. However, material No. 59 is unable to delete failed elements. To improve accuracy of simulation, material failure was modelled using MAT_ADD_EROSION, which allowed elements to be deleted when the effective plastic strain exceeded the defined value. The indenter and supports were modelled as rigid bodies using *MAT20 (rigid). To simulate the effect of screw joints, spot-welds are defined using beam elements with outer diameter of 4 mm.

Table 1. Material properties of ST14 sheet metal.

Density	E (GPa)	v	Yield (MPa)
7.83E+03	1.92E+02	0.3	170

Table 2. Material Properties of glass/epoxy composite laminate [20].

Density	E ₁	E ₂	E ₃	v _{1,2}	v _{1,3}	v _{3,2}	
1.48E+03	23.5	23.5	10.5	0.193	0.39	0.39	
G _{1,2}	G _{1,3}	G _{3,2}	XC	XT	YC	YT	SC
2.95	2.14	2.14	214	458	214	458	36

Contact between spot-welds and beam elements are defined using TIED_SHELL_EDGE_TO_SURFACE and contact AUTOMATIC_SURFACE_TO_SURFACE was employed to model the contact between the specimen and indenter and supports, without any tied nodes. The friction coefficient between the aluminum tube and steel indenter and supports was set at 0.5 (static and kinetic) [18, 19]. The numerically simulated models and the test set-up is shown in Figs. 8 & 9.

Where the nomination of each character is as below:

- E: Young's modulus, GPa,
- v: Poisson's ratio,
- G: Shear Stress, GPa,
- XC: Longitudinal compressive strength, MPa,
- XT: Longitudinal tensile strength, MPa,
- YC: Transverse compressive strength, MPa,
- YT: Transverse tensile strength, MPa,
- SC: Shear strength, MPa.

4. Results and Discussion

To determine the effects of composite reinforcements on flexural behavior of top-hat shaped hollow section beams, some specimens with different arrangements for the reinforcement are tested with three-point bending test apparatus. To confirm the accuracy of the results, 3 specimens were manufactured for each type and average of three-point bending curves are reported in each case. Load-displacement curves of reinforced and not-reinforced beams are presented in Fig. 10. Comparing diagrams of cases C1 and C0 in this Fig. shows that by applying fiber composite layer to the back-plate component, trend of the curve does not change significantly. Peak load in case C1 is decreased by 23% (Fig. 11) but total energy absorption, calculated by area under curve, is increased by 18.75% (Fig. 12). On the contrary, peak load is increased to a great extent in specimen C2. Results depict that in the case of fiber composite reinforcement through inner surface of hat-shaped bar, the elastic section of load-displacement curve is extended by 269% compared to case C0. The large amount of load reduction after peak load in specimen C2 is because of fiber breakages, rapid crack growth and also plastic hinge formation in metal section. In this case, total energy absorption is 4 times larger than specimen C0.

Using an extra composite component as reinforcement has caused a considerable change in trend of diagram representing specimen C3. In this case, peak load is reached in two stages. First stage, which is comparable to specimens C0 and C1, only illustrates the behavior of metal components and composite member is not involved. As the indenter proceeds, the composite reinforcement starts to get involved and load needed to continue bending is increased until the main peak load is reached.

A sudden drop in diagram of case C3 is noticed, right after the peak load, due to fiber breakage in middle of composite reinforcement and amount of load reduction is approximately equal to load increased in second stage of peak load.

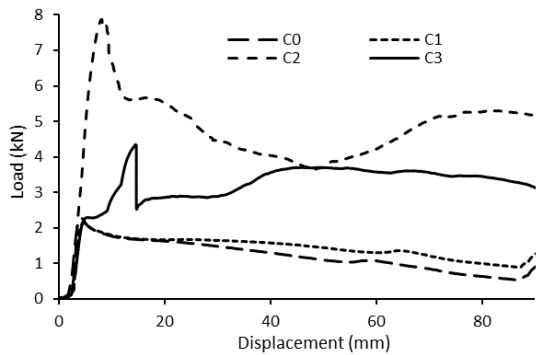


Fig. 10. Load-displacement diagrams of quasi-static three-point bending test.

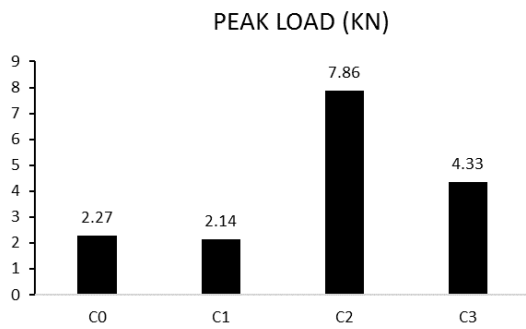


Fig. 11. Peak load of specimens.

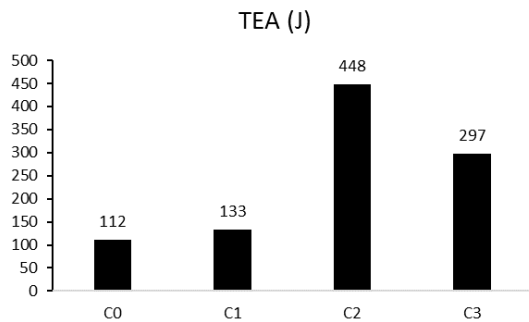


Fig. 12. Total Energy Absorption (TEA) of specimens.

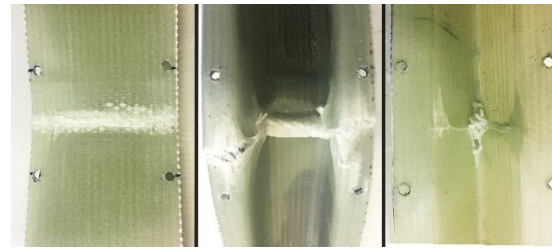


Fig. 13. Mechanism of collapse in composite-made sections.



Fig. 14. Folding pattern in experimental tests.

The sudden drop in load-displacement diagram of specimen C3 is justified by observing mechanism of collapse in composite-made sections due to their geometric specifications. Fig. 13 demonstrates that in specimens C1 and C2, fracture of epoxy matrix is developed as the indenter proceeds. Therefore, the damage has spread gradually. But in case of specimen C3, the crack growth has started from the tip of the triangle-shaped reinforcement and has resulted in rapid fiber breakages in straight lines. Consequently, the flexural resistance of the beam has decreased significantly at the moment. Unlike other cases, an upward trend is observed in diagram of C3 after primary fiber breakages. The reason could be explained by visual inspection of bending collapse mechanism. Folding pattern of specimens are compared in Fig. 14. As illustrated, dissimilar to cases C1 and C2, two extra plastic hinges are formed at sides of the main hinge during bending operation in specimen C3. Therefore, development of plastic deformation has required load increase thus energy absorption capacity is enlarged. Formation of extra side hinges are the result of specific cross-section employed in internal reinforcement. Fig. 15 explains process of deformation in specimen C3 during bending. The tip of triangle-shaped reinforcement prevents the sheet metal from folding toward inside the plastic hinge and as a result, material is pushed to the two sides of center hinge due to limited space and extra hinges are formed.



Fig. 15. Top-hat of specimen C3 from inside.

Furthermore, the parameter of Specific Energy Absorption (SEA) is also studied in specimens to consider the effect of lightweight design (Fig. 16). Comparison between SEA and total energy absorption shows that the gap between the amount of total absorbed energies have been influenced by considering weight of specimens in SEA parameter. For instance, quantity of total energy absorbed by specimen C2 is 51% higher than specimen C3. But considering SEA parameters, the value dedicated to case C2 is only 37% higher than case C3 due to lighter weight of specimen C2.

The numerical predictions of the energy absorptions for the three specimens are calculated and these values are used to compare with the results of experimental tests. The relative errors for FE simulations and tests are listed in Table 3. The load vs. displacement curves among the FE simulations and tests of the three specimens are compared in Figs. 17-19. It is revealed from Table 3 that the numerical values are in good agreement with the experimental values, and that the accuracy of the FE models are controllable within 4%. In addition, we can see from Fig. 20 that the final deformation patterns predicted by FE simulations agree well with the tests. Therefore, the established FE model is accurate enough and can be used to replace the physical test.

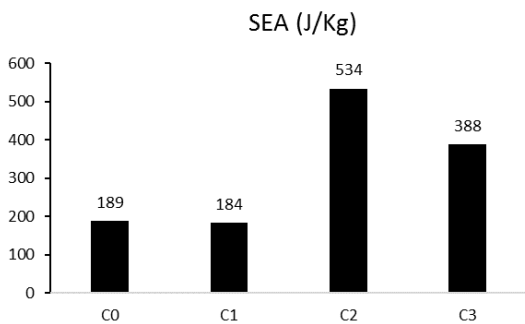


Fig. 16. Specific Energy Absorption (SEA) of specimens.

Table 3. Comparison of experimental and FE results of energy absorption.

Specimen	Experimental (J)	Numerical (J)	Error (%)
C1	132.63	137.67	3.83
C2	448.24	453.81	1.25
C3	297.19	296.59	0.20

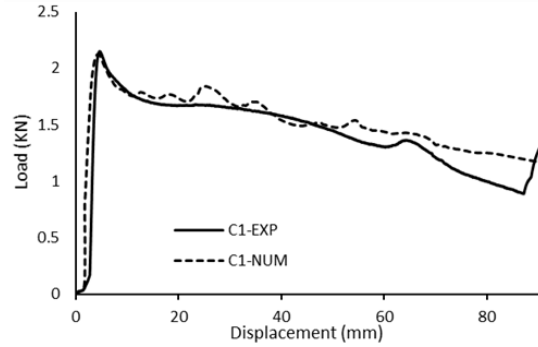


Fig. 17. Comparison of numerical and experimental results for specimen C1.

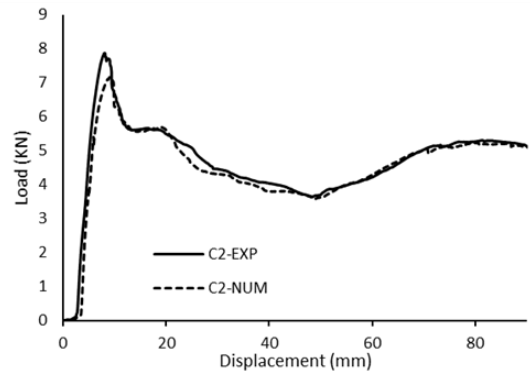


Fig. 18. Comparison of numerical and experimental results for specimen C2.

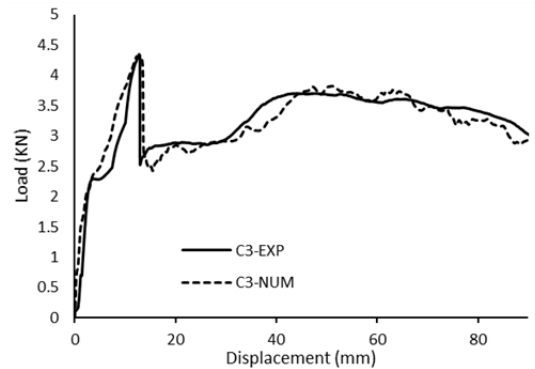


Fig. 19. Comparison of numerical and experimental results for specimen C3.

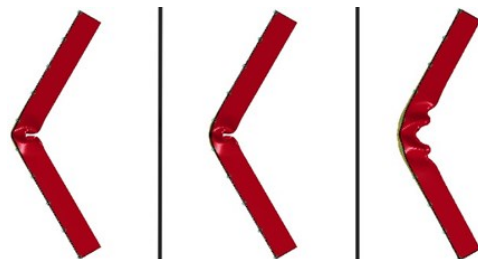


Fig. 20. Folding pattern in numerical simulations.

5. Conclusions

In this paper different methods of fiber composite reinforcement of a top-hat shape beam structure are investigated through experimental tests. The results show a significant improvement in strength and energy absorption capacity of the structure. As the absorbed energy is calculated by the area under load-displacement diagram, in a realistic elastic-plastic diagram, the amount of peak load is effecting the total energy absorption capacity. But the great portion of energy absorption is dependent on the average level of diagram between peak load and failure point. Since the main application of the studied beams are in automotive chassis structures, standard institutions have defined limits for intrusion. Meaning the energy of loading should be absorbed before reaching a specific length of deformation. Therefore, an increase in either peak load or the average load in plastic deformation stage is leading to more resistance and less intrusion. On the other hand, the load-displacement diagrams of quasi-static loadings are proved to present an acceptable estimation of the trend observed in the acceleration-displacement diagram of low-speed impacts like car accidents. Thus, any steep slope after diagram's peak load leads to a dangerous shock to the passengers. As a result, an ideal diagram for mentioned applications will include an acceptable amount of peak load which is smoothly transmitted into plastic deformation mode, similar to case C2 in this study. When the above results were taken into consideration, this study primarily yielded the following conclusions:

- The alternative approach, which was applied in case C3, have performed acceptably. However, despite the formation of two extra plastic hinges in the hat-section beam component, a considerable gap is observed between the amount of energy absorption in specimens C2 and C3. This result confirms the large energy absorbing capacity of fiber composite materials compared to a homogenous material such as steel.
- Performing reinforcing methods C2 and C3 has caused the energy absorption capacity to be risen by 300% and 165%, respectively. Therefore, applying reinforcement methods could significantly improve crashworthiness performance of a top-hat beam.
- No considerable improvement has occurred due to reinforcement method C1. Thus, if geometry is not a double-hat section beam and the back-plate is not curved, strengthening the plate would have a relatively low impact on the beam's flexural behavior.

References

- [1] Gui C., Bai J., Zuo W., 2018. Simplified crashworthiness method of automotive frame for conceptual design, *Thin-Walled Structures*, 131, pp. 324-335.
- [2] Santosa S, Banhart J, Wierzbicki T. 2001. Experimental and numerical analyses of bending of foam-filled sections, *Acta Mechanica*, 148, no. 1-4, pp. 199-213.
- [3] Hanssen A.G., Hopperstad O.S., Langseth M. 2000. Bending of square aluminum extrusions with aluminum foam filler, *Acta Mechanica*, 142(1), pp. 13-31.
- [4] Choubini M, Liaghat GH, Pol M.H. 2015. Investigation of energy absorption and deformation of thin-walled tubes with circle and square section geometries under transverse impact loading, *Modares Mechanical Engineering*, 15(1), pp. 75-83.
- [5] Pirmohammad N, Liaghat GH, Pol M.H., Sabouri H. 2014. Analytical, experimental and numerical investigation of sandwich panels made of honeycomb core subjected projectile impact, *Modares Mechanical Engineering*, 14(6), pp. 153-164.
- [6] Niknejad A, Abedi M.M., Liaghat GH, Nejad M.Z. 2015. Absorbed energy by foam-filled quadrangle tubes during the crushing process by considering the interaction effects, *Archives of Civil and Mechanical Engineering*, 15(2), pp. 376-391.
- [7] Chen W, Wierzbicki T, Santosa S. 2002. Bending collapse of thin-walled beams with ultralight filler: numerical simulation and weight optimization, *Acta Mechanica*, 153(3), pp. 183-206.
- [8] Lee S. H., Kim H. J., Choi N. S. 2006. Bending performance analysis of aluminum-composite hybrid tube beams, *Key Engineering Materials*, pp. 769-774.
- [9] Haedir J, Bambach M. R., Zhao X. L., Grzebieta R. H. 2009. Strength of circular hollow sections (CHS) tubular beams externally reinforced by carbon FRP sheets in pure bending, *Thin-Walled Structures*, 47(10), pp. 1136-1147.
- [10] Jung D.W., Kim H.J, Choi N.S. 2009. Aluminum-GFRP hybrid square tube beam reinforced by a thin composite skin layer, *Composites Part A: Applied Science and Manufacturing*, 40(10), pp. 1558-1565.
- [11] Shin K. C., Lee J. J., Kim K. H., Song M. C., Huh J. S. 2002. Axial crush and bending collapse of an aluminum/GFRP hybrid square tube and its energy absorption capability, *Composite Structures*, 57(1), pp. 279-287.
- [12] Ebrahimkhani M, Liaghat GH, Ahmadi H. 2018. Simulation of crushing performance of composite energy absorber under impact loading using continuum damage mechanics approach,

- Modares Mechanical Engineering*, 17(12), pp. 505-513.
- [13] Shokrieh M.M., Tozandehjani M, Omid M.J. 2009. Effect of fiber orientation and cross section of composite tubes on their energy absorption ability in axial dynamic loading, *Mechanics of Composite Materials*, 45(6), pp. 567-576.
- [14] NCAC Finite element model archive. 2013. *National Crash Analysis Centre*, George Washington University.
- [15] Malmberg T. 1995. *Aspects of Similitude Theory in Solid Mechanics, Part 1: Deformation Behavior*, Karlsruhe: FZKA.
- [16] Reddy J. 2004. *An introduction to the finite element method*, New York: McGraw-Hill.
- [17] LSDYNA version 971 keyword user's manual. Livermore Software Technology. April 2012.
- [18] Blau P.J. 2008. *Friction science and technology: from concepts to applications*, CRC press.
- [19] Davis J.R. 1997. *Concise metals engineering data book*, ASM international.
- [20] Javid H., Liaghat G.H., Ahmadi H. 2019. Experimental investigation of stitching effect on impact behavior of hybrid composite laminates. *MSc Thesis*, Tarbiat Modares University, Iran.